Bayesian analysis of an epidemiologic model of plasmodium falciparum malaria infection in Ndiop, Senegal

Nicole Cancre, Adama Tall, Christophe Rogier, Joseph Faye, Ousmane Sarr, Jean-François Trape, André Spiegel, Frédéric Y. Bois

▶ **To cite this version:**

Nicole Cancre, Adama Tall, Christophe Rogier, Joseph Faye, Ousmane Sarr, et al.. Bayesian analysis of an epidemiologic model of plasmodium falciparum malaria infection in Ndiop, Senegal. American Journal of Epidemiology, 2000, 152 (8), pp.760-770. 10.1093/aje/152.8.760 . ineris-00961851

HAL Id: ineris-00961851

https://ineris.hal.science/ineris-00961851

Submitted on 20 Mar 2014

HAL is a multi-disciplinary open access archive for the deposit and dissemination of scientific research documents, whether they are published or not. The documents may come from teaching and research institutions in France or abroad, or from public or private research centers.

L'archive ouverte pluridisciplinaire **HAL**, est destinée au dépôt et à la diffusion de documents scientifiques de niveau recherche, publiés ou non, émanant des établissements d'enseignement et de recherche français ou étrangers, des laboratoires publics ou privés.

BAYESIAN ANALYSIS OF AN EPIDEMIOLOGICAL MODEL OF *P. FALCIPARUM* MALARIA INFECTION IN NDIOP, SENEGAL

NICOLE CANCRE[1,2], ADAMA TALL[1],

CHRISTOPHE ROGIER[3], JOSEPH FAYE[1], OUSMANE SARR[1],

JEAN-FRANÇOIS TRAPE[4], ANDRE SPIEGEL[1], FREDERIC BOIS[2,5]

ABBREVIATIONS:

CI_{95}: 95 percent confidence interval

CV: coefficient of variation

AUTHORS' AFFILIATION:

[1] Institut Pasteur de Dakar, Dakar, Senegal

[2] B3E - INSERM U444, Faculté de Médecine St Antoine, Paris, France

[3] IMT-SSA, Marseille, France

[4] ORSTOM, Dakar, Senegal

[5] INERIS, Verneuil en Halatte, France

CORRESPONDENCE:

Dr. Frédéric Bois,
B3E - INSERM U444,
Faculté de Médecine St Antoine,
27 rue Chaligny,
75012 Paris - FRANCE
phone: 33 1 44 73 84 46
fax: 33 1 44 73 84 62
email: bois@b3e.jussieu.fr

RUNNING HEAD:

BAYESIAN ANALYSIS OF A MALARIA TRANSMISSION MODEL

ABSTRACT

Plasmodium falciparum has a complex transmission cycle. Public health planning and research would benefit from the ability of a calibrated model to predict the epidemiological characteristics of populations living in areas of malaria endemicity. This paper describes the application of Bayesian calibration to a malaria transmission model using longitudinal data gathered from 176 subjects in Ndiop, Senegal, from July 1 1993 to August 1 1994. The model is able to adequately predict *P. falciparum* parasitaemia prevalence in the study population. Further insight is provided into the dynamics of malaria in Ndiop: During the dry season, the estimated fraction of nonimmune subjects goes down to 20 percent and then increases up to 80 percent. The model-predicted time-weighted average incidences contributed by nonimmune and immune individuals are respectively 0.52 and 0.47 cases/day. The median times it takes to acquire an infection (conversion delay), for nonimmune and immune individuals, are estimated at 39 days and 285 days, respectively.

KEYWORDS: *MALARIA*, *MATHEMATICAL MODEL*, *BAYESIAN*, *PLASMODIUM FALCIPARUM*, *AFRICA*.

Malaria-induced mortality and morbidity are increasing worldwide (1). New orientations for control of the disease are emphasizing reduction in mortality and morbidity rather than eradication (2, 3) . Particular attention is given nowadays to development of vaccines. For scientists seeking to isolate potential vaccines, for clinicians evaluating vaccine safety and efficacy, and for public health managers developing malaria control programs, it is important to know the epidemiological characteristics of the disease and of the populations living in areas of endemicity. For example, in clinical trials organized to test the efficacy of potential vaccines, ways to minimize the proportion of non-susceptible, eventually immune, recruited subjects would improve statistical power.

However, malaria is a complex disease. *P. falciparum* infection confers only labile and partial immunity: acquisition of such an immunity only reduces the incidence of clinical malaria attacks without preventing infection (4-7), an infected subject may acquire a new infection before recovering from a previous one (a phenomenon known as "superinfection") (8), immunity is slowly acquired and function of exposure to infecting mosquitoes (9). To further complicate the problem, exposure to infectious mosquito bites is difficult to measure (10). Practically, exposure cannot be assessed for each subject, and all individuals are usually considered identically exposed; this constitutes a potential confounding factor for acquisition of immunity. The presence of parasites in individuals gives little information on exposure because parasitaemia can last a long time in the absence of treatment (11). Finally, in some geographic areas, exposure shows marked seasonality and can be very different from one year to the next (4).

An epidemiological model, accounting for these complexities, would be a useful tool to describe the dynamics of malaria and assess the epidemiological status of exposed populations (12), answering both the needs of public health planning and malaria research. Among the relevant models reported in the literature (8, 12-25), few have been statistically calibrated (*i.e.*, formally confronted to data) because of a lack of extensive longitudinal data and adequate statistical techniques. In only two cases (16, 21), 3 or 4 of the model parameters were estimated through minimization of χ^2 or G^2 (akin to entropy) criteria of fit. Simulation results from these models have never been presented with confidence intervals allowing an assessment of their reliability. Newly developed Bayesian numerical techniques (e.g., Markov chain Monte Carlo, MCMC, methods) (26-28) offer the possibility of an extensive statistical treatment of

complex epidemiological models, including inference about model parameter values, confidence intervals on model predictions, model checking and hypothesis testing. We apply these techniques to the malaria model described by Struchiner et al. (23). This model embodies a series of coherent, plausible, research hypotheses about *P. falciparum* malaria natural history and offer a synthesis of previous works by MacDonald (8), Dietz et al. (16), and Nedelman (21). We use MCMC simulations to fit the model to longitudinal data gathered from the village of Ndiop, in a meso-endemic area of Senegal. Model simulations of the underlying infection dynamics are presented.

MATERIALS AND METHODS

Population and data

The data used were gathered in the village of Ndiop (13°41'N, 16°23W) in the Sahelo-Soudanian region of Senegal. Since 1993, a longitudinal study has been conducted in Ndiop, in which data about entomological, parasitological and clinical data were collected. This analysis used data gathered from July 1 1993 to July 31 1994. The cohort follow-up was particularly intense from July to October 1993, when the prevalence of *P. falciparum* parasitaemia was highest. The rainy season usually lasts from June to October.

Human data. Only the 176 villagers (over a total of 396) who were continuously present in the village during the study period were included. Exclusions can be considered random with respect to exposure (in particular, it is very unlikely that people left the village because of mosquito bites, or to get treatment elsewhere) and no bias should be introduced by the removal of the traveling villagers. On the other hand, traveling villagers had unmeasured exposure to mosquitoes during their outings, and could have introduced bias if included. A local medical care unit was created to support the study after reaching an agreement with the population of the village and the public health authorities. Informed consent was obtained individually from the participants, or from their parents (for children); approval was obtained from the Ministère du Plan et de la Coopération and from the Ministère de la Santé Publique. The unit was provided with basic equipment for malaria diagnosis. A team of four physicians, two technicians and

four field workers, stationed in the village, was in charge of the contacts with the community and clinical follow-up. They were all trained in the clinical and laboratory diagnosis of malarial infection. Active surveillance consisted of: (i.) daily visit to each villager at home, to record body temperature and clinical symptoms of any nature having occurred during the previous 24 hours; (ii.) collection of thick blood smears (TB) once a week from July to October 1993, and once a month from November 1993 to August 1994. Passive surveillance included collection of TBs from subjects reporting to the health unit for any occasion. Special attention was paid to the use of anti-malarial drugs in the community and the population was asked not to use any such drugs without prescription. The only anti-malarial drug used was quinine (Quinimax; Sanofi-Labaz, Paris, France) administered at a dose of 25 mg/kg/day for 7 days in the following cases: children under 10 years old with fever (temperature higher than 38°C) and high parasitaemia (over 30 trophozoites per 100 leukocytes), pregnant women with clinical symptoms suggestive of malaria, persons with fever and very high parasitaemia (over 200 trophozoites per 100 leukocytes) and persons with severe malaria symptoms (coma, etc.)

A total of 5736 TBs were collected from the 176 villagers studied. To study the natural evolution of parasitaemia without interference with antimalarial treatments, TBs collected within 15 days after beginning treatment were excluded from the analysis. As a result, only 5000 TBs were considered in our analysis. All smears were double-read, once in the field by the technicians, and by an expert microscopist at the ORSTOM's laboratory in Dakar, whose reading was definitive. Slides were stained using 4 percent Giemsa's stain and up to 200 microscopic oil-immersion fields were examined at magnification 100. Parasite asexual stage (trophozoites) densities were reported as parasite count for 100 leukocytes (detection limit: 0.01 trophozoites for 100 leukocytes). The number, $D(t)$, of trophozoite-positive TBs on any given day for which subjects were seen, given the total number of TBs examined, $M(t)$, constituted an single data point. The whole data set will be noted **D** in the following. The observed prevalence presented on figure 2 were obtained by dividing $D(t)$ by $M(t)$ at each time t. Table 1 gives the distribution of subjects, positive TBs, and total TBs examined, by age and sex.

Mosquito data. The main anopheline species in Ndiop are *Anopheles arabiensis* and *An. gambiae*. They both contribute to the high endemicity of *Plasmodium falciparum* malaria (29). Captures at night of

mosquitoes attracted to human volunteers were used for sampling mosquito populations. Adult mosquitoes were captured on 12 humans for 3 consecutive nights each month from July to November 1993, and then weekly on 4 humans. Hourly human-bait collections were made on adult volunteers from 19:00 to 7:00. The volunteers were always placed at the same locations in the village, half of them indoors and the other half outdoors. Infectivity of captured mosquitoes for *P. falciparum* was assessed by detection of circumsporozoite antigen protein (CSP) with enzyme-linked immunosorbent assays (ELISAs) (30, 31). The number of infected mosquito bites per person (entomological inoculation rate, EIR, $h_e(t)$) was hence obtained for each collection day.

Dynamic model

The deterministic compartmental model developed by Struchiner et al. (23) was used to describe the natural history of the infection in humans. A brief summary is given here, since the model has been described elsewhere in full details (23, 32, 33). The model equations and the definition of each parameter are given in Appendix.

The human population is divided into four epidemiological classes or compartments (figure 1): nonimmune and immune negative subjects, in proportions $X_1(t)$ and $X_3(t)$, respectively; nonimmune and immune positive subjects, in proportions $Y_2(t)$ and $Y_3(t)$, respectively. Those proportions are time-varying and the model can predict their full time-course. Nonimmune positive subjects infectious to mosquitoes, in proportion $Y_1(t)$, are the subset of the nonimmune positives showing sexual stages (gametocytes) parasitaemia. It is assumed that immunity does not totally protect against infection, but reduces the probability of becoming infected. Individuals are deemed positive if they show trophozoite parasitaemia (as assessed by TB examination). For our study the birth and death rate, δ, was equal to zero.

Nonimmune negative individuals receive effective inoculations, in a proportion b_1 of the EIR, and become infected. They shows positive parasitaemia after an incubating period of N_1 days. An infected person may either acquire immunity or return to the nonimmune negative state. The maximum limiting rate at which immunity can be acquired is α_2. Immune positive individuals are not infectious to

mosquitoes and recover more quickly than nonimmune. Immune negative individuals receive inoculations, in a proportion b_2 of the EIR resulting in infection. The model specifies that $b_2 < b_1$. Immune negative individuals can lose their immunity if they receive no "booster" inoculation within the time interval τ. Immunity-boosting inoculations are a proportion f of the EIR. Such inoculations prolong an already acquired immunity but do not lead to an established brood of parasites.

An effective inoculation by an infectious mosquito produces one brood of parasites within the human host. Different mosquito bites can each inject a brood into an individual, and those broods are cleared independently of each other. We did not model the mosquito part of the parasite cycle: the EIR defined in the Struchiner model was replaced by our measurements, linearly interpolated.

Assuming all subjects, at $t = 0$, to be nonimmune and negative ($X_1(0) = 1$) is not realistic for Ndiop. However, neither initial conditions nor the actual "initial time" are known *a priori*. Preliminary simulations showed that, when starting with realistic conditions, equilibrium is reached in about two and half years. In that period of time, the system has also practically lost memory of its initial state. Consequently, the initial time was chosen to be December 22 1990. To acknowledge uncertainty in their values, the initial proportions of individuals in the compartments and initial average numbers of broods in individuals were considered as parameters to estimate. To respect the constraint of the summation to 1 of the initial proportions, the reparameterization given in appendix (eqs. 17-19) was used. No data on EIR were available from December 22 1990 to July 1 1993, before the beginning of parasitological monitoring. To supply realistic weekly values in input to the model during that period, we used the average of the values recorded in Ndiop from July 1993 to December 1996 for each week.

The model differential equations are nonlinear and include delays. They were integrated numerically, using the "Lsodes" algorithm provided by the MCSim software, version 4.2 (34). For given parameter values, integration of the equations given in appendix gives the time courses of its variables ($X_1(t)$, $X_3(t)$, $Y_1(t)$, $Y_2(t)$, $Y_3(t)$, $z_1(t)$, $z_2(t)$, $z_3(t)$) over any period of time starting December 22 1990. The sum, $\tilde{Y}(t)$, of $Y_2(t)$ and $Y_3(t)$ is a model-computed estimate of the instantaneous prevalence of *P. falciparum* parasitaemia in humans.

Statistical computations

A Bayesian approach was used to calibrate the model using the counts of *P. falciparum* trophozoite-positive TBs in Ndiop (the data, **D**). Basically, each model parameter (see the list in table 2 and in appendix), θ_i, was considered as a random variable and assigned a independent prior distribution, $p(\theta_i)$. Those distributions were updated together to yield a joint posterior distribution, $p(\boldsymbol{\theta}|\mathbf{D})$, such that model-computed time courses of prevalence (using parameter values drawn from that joint posterior) would be compatible with the data. According to Bayes' rule, $p(\boldsymbol{\theta}|\mathbf{D})$ is proportional to the product of the prior distributions by the data likelihood, $p(\mathbf{D}|\boldsymbol{\theta})$, under the model (35, 36).

The prior distributions summarize our knowledge about parameter values before seeing the Ndiop data (table 2). *A priori* lognormal or truncated lognormal distributions were assigned to several parameters. Their geometric means were set on the basis of the literature (4, 9, 11, 12, 21, 23). Their standard deviations (SD) were set by us to large values corresponding to a factor 5 or 2 (the latter for time delays, for which we had *a priori* better information), with eventual truncation when ranges were suggested by the literature. Uniform distributions over feasible or large regions were assigned in the absence of prior information, in particular for the initial state variables ($X_3(0)$, $z_1(0)$, $z_2(0)$ and $z_3(0)$) or their deconstraining parameters ($F_{Y_2(0)}$ and $F_{Y_3(0)}$).

To define the data likelihood, the observed number, $D(t)$, of trophozoite-positive TBs at time t was assumed to be binomially distributed with parameters $\tilde{Y}(t)$, the model-predicted prevalence ($0<\tilde{Y}(t)<1$), and $M(t)$, the total number of TBs counted at t. The joint posterior is therefore of the form:

$$p(\boldsymbol{\theta} \mid \mathbf{D}) \propto \prod_i p(\theta_i) \cdot \prod_t \left(\tilde{Y}(t)^{D(t)} \cdot \left(1 - \tilde{Y}(t)\right)^{M(t) - D(t)} \right) \qquad (1)$$

Unfortunately, because the dynamic model is nonlinear, there is no known analytical form for $p(\boldsymbol{\theta}|\mathbf{D})$. It is impossible to describe it and report inference about the parameters in a direct way. It remains possible to summarize that distribution by drawing random sets of parameters values using Metropolis sampling (26). This iterative procedure belongs to a class of MCMC techniques which has recently received much interest (for review see 27, 37-39). Briefly, algorithm was as follows: At the start

of a sampling "chain", all parameters were assigned values sampled from the priors. For any following iteration of the sampler, each component, θ_i, of the parameter vector was eventually updated by drawing a "proposed" new value, θ_i', out of a Gaussian "proposal" distribution centered on θ_i. Values of the joint posterior density at θ_i and θ_i' were then computed using equation 1 (this required running the differential model to obtain all needed values for $\tilde{Y}(t)$). Label the two obtained density values π and π'. If the ratio π'/π exceeded 1, the new value θ_i' was accepted and replaced θ_i; Otherwise, θ_i' was accepted only with probability π'/π. In case of rejection of θ_i' the value θ_i was kept. After updating (eventually) all model parameters sequentially (the updating order does not matter in the long run), their values were recorded, therefore completing one iteration of the chain. Iterations were performed until the chain had reached equilibrium, *i.e.*, until all parameters had approximately converged in distribution to $p(\theta|\mathbf{D})$. The SD of the proposal Gaussian was adjusted periodically to yield an acceptance rate of 25% (40). The convergence of several Markov chains to $p(\theta|\mathbf{D})$ was assessed using Gelman and Rubin's $\hat{R}$ diagnostic (41). The parameter sets recorded after equilibrium was reached, were used to form histograms or compute summary statistics of the posterior distributions for estimands of interest (*e.g.*, marginal parameter distributions, combinations of parameters, or model predictions). Obtaining the posterior distribution of model predictions required running the malaria model once for each parameter set recorded. All the above computations were performed by the MCSim software, version 4.2 (34).

RESULTS

Model fit

Convergence of three independent MCMC chains was reached after about 40,000 iterations ($\hat{R}$ diagnostic at 1.07 on average, ranging from 1 to 1.2). Fifteen thousand parameter sets were sampled, by keeping 1 out of every 6 iterations from an additional 30,000 of each chain (each iteration kept yielded a parameter set). All simulations and inferences presented in the following were made using this final sample from $p(\theta|\mathbf{D})$.

A good fit to the data was obtained, while maintaining scientifically plausible parameter values. Figure 2 shows the daily trophozoite parasitaemia prevalences ($D(t)/M(t)$) together with the corresponding model predictions, $\tilde{Y}(t)$, made with the parameter set having highest posterior density in the final sample. This model prediction is the "best" of all, but is also quite representative of the set. Ten others model-predicted time courses of prevalence are presented, obtained using parameter vectors randomly drawn from $p(\boldsymbol{\theta}|\mathbf{D})$. The differing model trajectories for all these curves reflect uncertainty in model predictions. However, they all have similar behavior. The posterior 95% confidence interval on predictions is also displayed. The rise to the peak (from about 20 percent prevalence, up to 70 - 80 percent) is somewhat jagged and mostly driven by the random biting rate of mosquitoes. The subsequent decrease is smoother and driven by the gradual recovery of the infected subjects in the dry season. Prevalence returns to about 20 percent at the end of the dry season. Running a standard smoothing curve through the data would be purely descriptive and would give no insight about the underlying dynamics. Our goal is not so much to "fit" the data than to extract, from them, information about the model parameters.

Posterior parameter distributions

The joint posterior distribution of all parameters can be viewed in several dimensions, but for simplicity only the marginal distribution of each parameter is described here. Table 3 summarizes these distributions on the basis of the final parameter sample. For all biological parameters, the posterior location is noticeably different from the corresponding prior mean. Posterior standard deviations are much lower than *a priori* specified (compare tables 2 and 3) because important information about those parameters has been extracted from the data.

The median sojourn time ($1/r_1$) of a parasite brood in nonimmune human hosts is about 200 days (CI_{95} 18- 2000 days). Albeit lower, this is still compatible with the 850 days previously assumed (9, 21, 23). For immune subjects this sojourn time is 19 days (with a 30 percent CV and CI_{95} 11 - 30 days). Immunity appears to affect the life span of the parasite in human hosts.

The recovery rate from infectiousness to mosquitoes among nonimmune positive hosts (α_1) is high but poorly identified. It corresponds to a median half life of 6 days, with CI_{95} 0.5 - 125 days. The window of infectivity is therefore quite small (as expected from the relative brevity of the prevalence peak during the year).

As indicated by the median value of α_2, about 210 days (1/0.0047) are at least necessary for a human host to acquire immunity to *P falciparum*. This estimation is quite precise (CV of about 10 percent) and much lower than the *a priori* value. Simulations indicate that for an inhabitant of Ndiop, exposed to a seasonal meso-endemic transmission, the numbers of infectious and noninfectious parasite broods present at any time in nonimmune hosts (z_1 and z_2) average around 10 (data not shown). In such conditions (see eq. 13 of the appendix) the actual immunity acquisition delay (A_1) is equal to 214 days on average, close to its minimum value. Immunity appears more quickly than *a priori* expected, but still takes at least half a year to be in effect.

The interval of time, τ, until an immune host loses immunity in the absence of exposure to infectious mosquito bites is about 230 days (CI_{95} 180 - 290 days). The incubation period, N_1, lasts on average 22 days (CI_{95} 15 - 28 days).

Few infectious bites (f is about 3 percent) are able to boost immunity, and this boosting does not seem to be very important, *a posteriori*. The proportion of potentially infectious bites actually resulting in an infection is much higher in nonimmune hosts (b_1 = 40 percent, CI_{95} 26 percent - 91 percent) than in immune subjects (b_2 = 2.5 percent, CI_{95} 1.5 percent - 3.5 percent). Immunity, although progressively acquired, seems to efficiently protect from infection.

The marginal posterior distributions of the sampled initial state variables or their reparameterizations ($X_3(0)$, $F_{Y_2(0)}$, $F_{Y_3(0)}$, $z_1(0)$, $z_2(0)$, and $z_3(0)$) are very close to the corresponding priors. This shows the insensitivity of the model to those parameters: their values do not appreciably affect the results.

Model predictions of the underlying dynamics

After fitting, the model can be used to simulate various scenarios to better understand the dynamics of *P. falciparum* infection in our study population. Figure 3 shows predictions of time-course of malaria immunity status during the year of our study and the following wet season (July 1993 to December 1994), together with the measured EIR. At the end of the dry season, the population composition is as follows: 63 percent (CI_{95} 35 - 85) nonimmune negative (X_1), 12 percent (CI_{95} 10 - 15) nonimmune positive (Y_2), 1 percent (CI_{95} 0.7 - 2) immune positive (Y_3), and 24 percent (CI_{95} 5 - 50) immune negative (X_3). These proportions vary from year to year as mosquito as biting fluctuates in timing and intensity. Nonetheless, some behaviors appear stable. The proportion of nonimmune negative falls very quickly, and practically to zero, as soon as mosquito biting increases. Infected subjects initially transfer to a nonimmune positive status, whose proportion reaches a peak at about the same time as the biting rate (with a short delay imposed by incubation). Nonimmune positive subjects then transfer mostly to the immune status. However, the fraction of immune positive individuals does not increase much and individuals quickly eliminate parasites to become immune negative. Near the end of the dry season immune negative individuals loose immunity and the fraction of nonimmune negative increases quickly. Overall, most subjects move through the four states as the year progresses.

Other epidemiological data point to the dependence of immunity on continued exposure (9). For example, in a malaria control program consisting in insecticide spraying against mosquitoes and mass antimalarial treatment of the human population for two wet seasons, malaria prevalence during the subsequent wet season was higher than in a control population; the following year, in the absence of intervention, prevalence became similar for the two populations (9). This behavior, also discussed by Halloran et al. (32), is reproduced by the present model (data not shown).

The incidence of malarial infection is difficult to measure, since it requires identification of new infections in potentially already parasitaemic individuals. The model can easily gives an estimate for various incidence rates. Figure 4 presents the model-reconstructed instantaneous incidence rates (number of new cases/day) of trophozoite parasitaemia contributed by nonimmune and immune individuals during

the 1993 wet season in Ndiop (incidence was null during the dry season). These rates correspond to the products $\lambda_1(t) \infty X_1 \infty 396$ and $\lambda_2(t) \infty X_3 \infty 396$, respectively (396 being the total size of the population of Ndiop). The time-weighted average incidences, over the year, contributed by nonimmune and immune individuals are about the same — respectively 0.52 (CI_{95} 0.40 - 0.63) and 0.47 (CI_{95} 0.30 - 0.67) cases/day. However, the incidence time profiles for these two sub-populations do differ. Early incident cases are contributed mostly by nonimmune individuals, and late cases by immune subjects. This is explained by the progressive decline of the nonimmune negative population as the wet season progresses (figure 3). For the whole population, the time-weighted average is estimated at 0.99 (CI_{95} 0.87 - 1.2) cases/day.

Figure 5 gives the immunity acquisition delay and the conversion delays for nonimmune and immune subjects as a function of the EIR. These delays are time-dependent when EIR varies (see eqs. 9 and 10 in appendix). To avoid this time dependency, the model predictions presented here were computed with constant EIRs. Computations were made with the parameter set having highest posterior density. When biting is seasonal, as in Ndiop, the curves in figure 5 can still be used to compute approximate delays given yearly average EIRs. The immunity acquisition delay ($1/A_1$) first decreases proportionally to inoculation rate. It starts flattening at 0.01 bites per person per day. After that point, it remains at a minimum value of about 210 days (equal to $1/\alpha_2$). The conversion delays are the average time it takes a disease-free individual to acquire an infection. They are given by $N_1+1/\lambda_1(t)$ and $N_1+1/\lambda_2(t)$ for nonimmune and immune subjects, respectively. At low inoculation rates (at least below the Ndiop average of 0.1 potentially infectious bites/person/day), the conversion delay is about 16 times (ratio b_1/b_2) lower for immune than for nonimmune subjects. These delays first decrease proportionally to inoculation rate and, as it increases, they tend toward a common minimum: the incubation period. For a nonimmune individual, the median estimate of the conversion delay, in 1993 in Ndiop, was 39 days (CI_{95} 29 - 46). For an immune subject it was equal to 285 days (CI_{95} 205 - 440). The 95% confidence bands for all delays presented in figure 5 span approximately a factor 2.

DISCUSSION

This work demonstrates the possibility to statistically calibrate a complex mathematical model with epidemiological data, using a Bayesian framework. As a result, a reasonable fit of the parasitaemia prevalence data was reached, showing that the model is compatible with the observations, and a sample of model parameters values was obtained from their joint posterior distribution. The model was then used to predict quantities otherwise difficult to measure, given the current state of knowledge. We obtained, for example, estimates of instantaneous and average incidence rates of *P. falciparum* parasitaemia. Among the statistical methods available to us, Bayesian updating is particularly appropriate for integrating two forms of information (28, 42, 43): "prior knowledge" from the scientific literature, and "data" from field studies. Still, several issues can be discussed about the data used, the structure of the chosen model, and various assumptions we made.

The data were obtained through an intensive follow-up. A potential bias in subject recruitment arises as individuals were offered the opportunity to present themselves to clinical examination. *P. falciparum*-infected individuals presenting symptoms may have been over-represented. However, blood samples were analyzed in all self-motivated visits, related or not to malaria, and only 16 percent of the samples analyzed where obtained during such visits. We also verified, through examination of residuals after model calibration, that the prevalence of *P. falciparum* parasitaemia in self-motivated consultations was not higher than in systematic screenings. The impact of a potential bias in self-motivated consultations should therefore be small or nonexistent. We only analyzed data on the prevalence of *P. falciparum* trophozoites parasitaemia, but it would also be interesting to extend the model to consider data on the number of clinical malaria attacks.

The model developed by Struchiner et al. (23) offers a reasonable, even if simplified, description of malaria physiopathology. We did not include the original description by Struchiner et al. of the parasite cycle in mosquitoes. That was not needed since our data included EIR throughout the year. However, that rate was assumed to be precisely measured and identical for all subjects. This assumption was needed because the full treatment of "error in variables" problems is difficult in the context of large

and computationally intensive models. Another important set of modeling assumptions concerns immunity. In the model, an infected person does not necessarily acquire immunity after one inoculation and immunity can be lost with time. Although the hypothesis of a definitive acquisition of immunity to the different antigenic strains of parasite seen during an individual's lifetime (18) is not explicitly considered, the model does assume that the acquisition of immunity is a function of the number of co-infecting strains.

Our analysis was performed by pooling data on all subjects (but still preserving the longitudinal aspect of the data at the population level). This could be improved by taking into account the age structure of the population, for example through a hierarchical statistical model (44). This could shed light of on age-related differences in susceptibility to *P. falciparum* infection. At this occasion, it might be possible to take into account the fact that the feeding behavior of mosquitoes is affected by a number of host- or environment-related factors (45-48).

According to the model, in conditions similar to those of Ndiop, the fraction of susceptible subjects is the highest at the very end of the dry season, when mosquitoes start biting again. This makes sense given what is known of the natural history of malaria. The advantage of using a calibrated model, assuming it is correct or sufficiently robust, is that it offers a quantitative estimate of this fraction and of the associated uncertainty. Use of such information in vaccination trial design can help assess and improve statistical power. Power calculations show that the effective size of a trial is proportional to the fraction of susceptible subjects (e.g., a study with 10000 person-days and 50 percent susceptible subjects in each group has the same power as a 5000 person-days, 100 percent susceptible, study). Location-specific EIRs could be used in input to the model to assess the best time of the year for a study in other areas than Ndiop.

A dynamic perspective on malaria, as embodied in an epidemiological model able to disentangle time-varying exposures, superinfections, and complex immunity acquisition processes, is essential for a proper analysis of malaria field study data. Too many pitfalls of confounding and bias, difficult to avoid, await standard data analyses. The model analyzed here is by no means complete or perfect, but it offers a reasonable basis for extension and improvement. Several research teams, worldwide, are currently trying

to improve malaria models. These efforts would benefit from the statistical techniques presented here. Calibrated models can be powerful predictive tools for experimental design and exploration of public health measures.

ACKNOWLEDGMENTS

We wish to acknowledge the administrative and technical support of the Institut Pasteur and ORSTOM in Dakar, and particularly the help of Mr. E.-H. Ba. We are grateful to the villagers of Ndiop and to the local study team for their collaboration. We also thank Dr K. Dietz, Dr. J. Eisenberg, Dr. D. Fontenille, Dr. O. Garraud, Dr. S. Gupta, Dr. L. Lochouarn for their helpful comments.

FINANCIAL SUPPORT

This work was supported by a grant from the Ministère de la Coopération et du Développement (Paris).

REFERENCES

1. World Health Organization (W.H.O). Activités antipaludiques: les 40 dernières années. World Health Statistics Quaterly 1988;41:64-73.
2. World Health Organization (W.H.O). WHO Expert Committee on Malaria: eighteenth report. Geneva: World Health Organization, 1986.
3. Najera JA. Malaria control: present situation and need for historical research. Parassitologia 1990;32:215-229.
4. Gilles HM, Warrell DA. Bruce-Chwatt's Essential Malariology. London: Edward Arnold, 1993.
5. Christophers SR. The mechanism of immunity against malaria in communities living under hyper-endemic conditions. The Indian Journal of Medical Research 1924;12:273-294.
6. Miller M. Observations on the natural history of malaria in the semi-resistant West African. Transactions of the Royal Society of Tropical Medicine and Hygiene 1958;52:152-167.
7. Garnham PCC. Malaria immunity in Africans: effects in infancy and early childhood. Annals of Tropical Medicine and Parasitology 1949;43:47-61.

8. MacDonald G. The analysis of infection rates in diseases in which superinfection occurs. Tropical Diseases Bulletin 1950;47:907-914.
9. Molineaux L, Gramiccia G. The Garki Project. Geneva: World Health Organization, 1980.
10. Smith T, Charlwood JD, Takken W, Tanner M, Spiegelhalter DJ. Mapping the densities of malaria vectors within a single village. Acta Tropica 1995;59:1-18.
11. Earle WC, Perez M, Del Rio J, Arzola C. Observations on the course of naturally acquired malaria in Puerto Rico. Puerto Rico Journal Public Health and Tropical Medicine 1939;14:391-406.
12. Anderson RM, May RM. Infectious diseases of humans: dynamics and control. Oxford: Oxford University Press, 1991.
13. Bekessy A, Molineaux L, Storey J. Estimation of incidence and recovery rates of *Plasmodium falciparum* parasitaemia from longitudinal data. Bulletin of the World Health Organization 1976;54:685-693.
14. Aron JL. Malaria epidemiology and detectability. Transactions of the Royal Society of Tropical Medicine and Hygiene 1982;76:595-601.
15. Aron JL. Mathematical modelling of immunity to malaria. Mathematical Biosciences 1988;90:385-396.
16. Dietz K, Molineaux L, Thomas A. A malaria model tested in African Savannah. Bulletin of the World Health Organization 1974;50:347-357.
17. Bailey NTJ. The Biomathematics of Malaria. London: Griffin & Compagny Ltd., 1982.
18. Gupta S, Trenholme K, Anderson RM, Day KP. Antigenic diversity and the transmission dynamics of *Plasmodium falciparum*. Science 1994;263:961-963.
19. Milligan PJM, Downham DY. Models of superinfection and acquired immunity to multiple parasite strains. Journal of Applied Probability 1996;33:915-932.
20. Dutertre J. Etude d'un modèle épidémiologique appliqué au paludisme. Annales de la Société Belge de Médecine Tropicale 1976;56:127-141.
21. Nedelman J. Inoculation and recovery rates in the malaria model of Dietz, Molineaux, and Thomas. Mathematical Biosciences 1984;69:209-233.
22. Nasell I. On superinfection in malaria. IMA Journal of Mathematics Applied in Medicine & Biology 1986;3:211-227.

23. Struchiner CJ, Halloran ME, Spielman A. Modelling malaria vaccines I: new uses for old ideas. Mathematical Biosciences 1989;94:87-113.
24. Dietz K. Mathematical models for transmission and control of malaria. In: Wernsdorfer WH, McGregor I, eds. Principles and practice of malariology. London: Churchill Livingstone, 1988:1091-1133.
25. De Zoysa APK, Mendis C, Gamage-Mendis AC, Weerasinghe S, Herath PRJ, Mendis KN. A mathematical model for *Plasmodium vivax* malaria transmission: estimation of the impact of transmission-blocking immunity in an endemic area. Bulletin of the World Health Organization 1991;69:725-734.
26. Smith AFM. Bayesian computational methods. Philosophical Transactions of The Royal Society of London - Series A 1991;337:369-386.
27. Gelman A. Iterative and non-iterative simulation algorithms. Computation and Scientific Statistics 1992;24:433-438.
28. Gelman A, Rubin DB. Markov chain Monte Carlo methods in biostatistics. Statistical Methods in Medical Research 1996;5:339-355.
29. Fontenille D, Lochouarn L, Diatta M, et al. Four years' entomological study of the transmission of seasonal malaria in Senegal and the bionomics of *Anopheles gambiae* and *A. Arabiensis*. Transactions of the Royal Society of Tropical Medicine and Hygiene 1997;91:647-652.
30. Wirtz RA, Zavala F, Charoenvit Y, et al. Comparative testing of monoclonal antibodies against *Plasmodium falciparum* sporozoïtes for ELISA development. Bulletin of the World Health Organization 1987;65:39-45.
31. Beier JC, Perkins PV, Koros JK, et al. Malaria sporozoite detection by dissection and ELISA to assess infectivity to Afrotropical Anopheles. Journal of Medical Entomology 1990;27:377-384.
32. Halloran ME, Struchiner CJ, Spielman A. Modelling malaria vaccines II: population effects of stage-specific malaria vaccines dependent on natural boosting. Mathematical Biosciences 1989;94:115-149.
33. Halloran ME, Struchiner CJ. Modeling transmission dynamics of stage-specific malaria vaccines. Parasitology Today 1992;8:77-85.

34. Bois FY, Maszle D. MCSim: a simulation program. Journal of Statistical Software 1997;2(9):http://www.stat.ucla.edu/journals/jss/v02/i09 (also available at ftp://sparky.berkeley.edu/pub/mcsim).
35. Bernardo JM, Smith AFM. Bayesian Theory. Chichester: John Wiley & Sons, 1994.
36. Gelman A, Carlin JB, Stern HS, Rubin DB. Bayesian Data Analysis. London: Chapman & Hall, 1995.
37. Gelfand AE, Smith AFM. Sampling-based approches to calculating marginal densities. Journal of the American Statistical Association 1990;85:398-409.
38. Gelfand AE, Smith AFM, Lee T-M. Bayesian analysis of constrained parameter and truncated data problems using Gibbs sampling. Journal of the American Statistical Association 1992;87:523-532.
39. Gilks WR, Richardson S, Spiegelhalter DJ. Markov Chain Monte Carlo in Practice. London: Chapman & Hall, 1996.
40. Roberts GO, Gelman A, Gilks WR. Weak convergence and optimal scaling of random walk Metropolis algorithms. The Annals of Applied Probability 1997;7:110-120.
41. Gelman A, Rubin DB. Inference from iterative simulation using multiple sequences. Statistical Science 1992;7:457-511.
42. Best NG, Spiegelhalter DJ, Thomas A, Brayne CEG. Bayesian analysis of realistically complex models. Journal of the Royal Statistical Society Series A 1996;159:323-342.
43. Givens GH, Hughes JP. A method for determining uncertainty of predictions from deterministic epidemic models. In: Anderson JG, Katzper M, eds. Proceedings of Health Sciences, Physiological and Pharmacological Simulation Studies - 1995 Western Multiconference. San Diego: Society for Computer Simulation, 1995:205-210.
44. Lange N, Carlin BP, Gelfand AE. Hierarchical Bayes models for the progression of HIV infection using longitudinal CD4 T-cell numbers. Journal of the American Statistical Association 1992;87:615-632.
45. Glynn J, Bradley D. Inoculum size, incubation period and severity of malaria. Analysis of data from malaria therapy records. Parasitology 1995;110:7-19.

46. Lindsay SW, Adiamah JH, Miller JE, Pleass RJ, Armstrong JRM. Variation in attractiveness of human subjects to malaria mosquitoes (diptera: culicidae) in the Gambia. Journal of Medical Entomology 1993;30:368-373.
47. Smith T. Proportionality between light trap catches and biting densities of malaria vectors. Journal of the American Mosquito Control Association 1995;11.
48. Tanner M. Kilombero malaria project. The level of anti-sporozoite antibodies in a highly endemic malaria area and its relationship with exposure to mosquitoes. Transactions of the Royal Society of Tropical Medicine and Hygiene 1992;86:499-504.

APPENDIX

The following equations, from Struchiner et al. (23), describe the transitions among model compartments:

$$\frac{dX^1(t)}{dt} = \delta(t) + R^1(t)Y^2(t) - (\lambda^1(t) + \delta(t))X^1(t) + \Delta^3(t) \quad (1)$$

$$\frac{dX^3(t)}{dt} = R^2(t)Y^3(t) - (\lambda^2(t) + \delta(t))X^3(t) - \Delta^3(t) \quad (2)$$

$$\frac{dY^2(t)}{dt} = \lambda^1(t)X^1(t) - \left[A^1(t) + R^1(t) + \delta(t)\right]Y^2(t) \quad (3)$$

$$\frac{dY^3(t)}{dt} = \lambda^2(t)X^3(t) + A^1(t)Y^2(t) - \left[R^2(t) + \delta(t)\right]Y^3(t) \quad (4)$$

$$\frac{dz^1(t)}{dt} = \lambda^1(t) - \alpha^1(t)z^1(t) \quad (5)$$

$$\frac{dz^2(t)}{dt} = \alpha^1(t)z^1(t) - r^1z^2(t) \quad (6)$$

$$\frac{dz^3(t)}{dt} = \lambda^2(t) - r^2z^3(t) \quad (7)$$

$$Y^1 = \frac{1 - e^{-}}{1 - e^{-} + } Y^2 \quad (8)$$

$$\lambda^1(t) = b^1h^{-}(t - N^1) \quad (9)$$

$$\lambda^2(t) = b^2h^{-}(t - N^1) \quad (10)$$

$$R^1 = r^1z^2 \frac{e^{-} + }{1 - e^{-} + } \quad (11)$$

$$R^{2} = r^{2}z^{3}\frac{e^{-}}{1-e^{-}} \tag{12}$$

$$A^{1} = \alpha^{?}(1-e^{-+}) \tag{13}$$

$$\Delta^{3}(t) = \left\{R^{2}(t-\tau)\cdot Y^{3}(t-\tau) + (f-b^{2})\cdot h^{e}(t-\tau-N^{1})\cdot X^{3}(t-\tau)\right\}e^{-+\delta'\tau} \tag{14}$$

with :

$$\bar{h}^{b} = \int_{t-\tau}^{t}\frac{h^{b}(u)}{\tau}\,du \tag{15}$$

$$h^{h}(t) = b^{?}\cdot h^{e}(t-N^{1}), \qquad b^{?} \le f \le 1 \tag{16}$$

$$Y^{3}(0) = F^{}(1-X^{3}(0)) \tag{17}$$

$$Y^{?}(0) = F^{}(1-X^{3}(0)-Y^{3}(0)) \tag{18}$$

$$X^{1}(0) = 1-X^{3}(0)-Y^{3}(0)-Y^{?}(0) \tag{19}$$

The symbols (in alphabetical order) used in the above equations and in the text correspond to:

A_1: rate at which immunity to *P. falciparum* infection is acquired by a human host.

b_1: proportion of bites by infectious mosquitoes on negative nonimmune hosts actually resulting in infection.

b_2: proportion of bites by infectious mosquitoes on negative immune hosts actually resulting in infection.

f: boosting factor (*i.e.*, proportion of bites by infectious mosquitoes on immune hosts resulting in boosted immunity).

$F_{Y_2(0)}$: deconstraining parameter for $Y_2(0)$.

$F_{Y_3(0)}$: deconstraining parameter for $Y_3(0)$.

$h_e(.)$: entomological inoculation rate (EIR): number of *P. falciparum* infectious bites per human per day.

N_1: *P. falciparum* parasitaemia incubation period in humans (in days).

r_1: rate constant of elimination of a brood of parasites by nonimmune positive hosts (in days^{-1}).

r_2: rate constant of elimination of a brood of parasites by immune positive hosts (in days^{-1}).

R_1: recovery rate for nonimmune positive individuals (in days^{-1}).

R_2: recovery rate for immune positive individuals (in days^{-1}).

X_1: proportion of nonimmune negative (*i.e.*, naive) individuals in the population.

$X_1(0)$: initial value (at time zero, *i.e.* December 22 1990) of X_1.

X_3: proportion of immune negative individuals.

$X_3(0)$: initial value of X_3.

Y_1: proportion of nonimmune positive individuals potentially infectious for mosquitoes.

Y_2: proportion of nonimmune positive individuals.

$Y_2(0)$: initial value of Y_2.

Y_3: proportion of immune positive individuals.

$Y_3(0)$: initial value of Y_3.

z_1: average number of infectious broods of parasite per nonimmune positive human host.

$z_1(0)$: initial value of z_1.

z_2: average number of noninfectious broods of parasite per nonimmune positive human host.

$z_2(0)$: initial value of z_2.

z_3: average number of noninfectious broods of parasite per immune positive human host.

$z_3(0)$: initial value of z_3.

α_1: recovery rate from infectiousness to mosquitoes among nonimmune positive hosts (in days^{-1}).

α_2: maximum rate at which immunity to *P. falciparum* infection can be acquired by a human host (in days^{-1}).

δ: death and birth rate in the human population (in days^{-1}).

Δ_3: daily fraction of immune negative subjects loosing immunity.

λ_1: infection rate for nonimmune negative subjects (probability per day for such a subject to be infected).

λ_2: infection rate for immune negative subjects (probability per day for such a subject to be infected).

τ: time delay needed for an immune host to loose immunity in the absence of exposure to infection (in days).

TABLE 1. Counts* of individuals and thick blood smear by sex and age in the cohort studied.

Sex	Age (years)						
	< 1	1-4	5-9	10-14	15-19	20-30	> 30
Female	5 (67/160)	9 (69/222)	15 (207/454)	14 (190/396)	8 (147/241)	15 (171/405)	21 (214/594)
Male	6 (52/192)	23 (265/719)	16 (220/485)	8 (106/178)	6 (106/149)	5 (65/168)	25 (265/637)

* Count of subjects in class (trophozoite-positive smears / total smears examined).

TABLE 2. Prior distributions adopted for the model parameters.

Parameter	Source	Distribution	Mean	Standard Deviation	Min	Max
r_1	(9, 21)	Lognormal	0.00118 *	5 †	—	—
r_2	(9, 21)	Lognormal	0.0134 *	5 †	—	—
α_1	(9, 21)	Lognormal	0.0108 *	5 †	—	—
α_2	(9, 21)	Lognormal	0.00026 *	5 †	—	—
τ	(9, 11, 12)	Truncated lognormal	365 *	2 †	90	1095
N_1	(4, 9)	Truncated lognormal	15 *	2 †	5	50
f	— ‡	Uniform	0.5	0.289	0	1
b_1	— ‡	Uniform	$(1+b_2)/2$	$(1-b_2)$/v12	b_2	1
b_2	— ‡	Uniform	$f/2$	f/v12	0	f
$X_3(0)$	— ‡	Uniform	0.5	0.289	0	1
$F_{Y3(0)}$	— ‡	Uniform	0.5	0.289	0	1
$F_{Y2(0)}$	— ‡	Uniform	0.5	0.289	0	1
$z_1(0)$	— ‡	Uniform	50	28.9	0	100
$z_2(0)$	— ‡	Uniform	50	28.9	0	100
$z_3(0)$	— ‡	Uniform	50	28.9	0	100

* Geometric mean.

† Geometric standard deviation (exponential of the SD in log space).

‡ Given the lack of prior information, uninformative uniform prior was used.

TABLE 3. Summary of the posterior (fitted) distributions for the model parameters.

Parameter	Median	Mean (SD)	Geometric mean (GSD*)	2.5th %tile	25th %tile	75th %tile	97.5th %tile
r_1	0.0049	0.030 (0.18)	0.0047 (3.3)	0.0005	0.0026	0.0082	0.057
r_2	0.053	0.055 (0.015)	0.054 (1.3)	0.033	0.045	0.063	0.095
α_1	0.12	0.33 (0.51)	0.12 (4.9)	0.0055	0.04	0.39	2.0
α_2	0.0047	0.0047 ($4.6\infty10^{-4}$)	0.0047 (1.1)	0.0037	0.0044	0.0051	0.0055
τ	230	235 (30)	230 (1.1)	180	220	260	290
N_1	22	22.5 (2.9)	22 (1.2)	15	21	24	27.5
f	0.030	0.038 (0.051)	0.032 (1.5)	0.019	0.026	0.035	0.076
b_1	0.39	0.43 (0.16)	0.41 (1.4)	0.26	0.33	0.48	0.91
b_2	0.024	0.024 (0.005)	0.023 (1.2)	0.015	0.021	0.027	0.035
$X_3(0)$	0.66	0.62 (0.26)	0.525 (2.0)	0.080	0.42	0.84	0.98
$F_{Y_3(0)}$	0.37	0.42 (0.28)	0.30 (2.7)	0.025	0.18	0.66	0.96
$F_{Y_2(0)}$	0.42	0.45 (0.27)	0.33 (2.6)	0.030	0.22	0.66	0.95
$z_1(0)$	51	50.5 (28)	39 (2.5)	3.7	27	74	96
$z_2(0)$	48	49 (28)	37 (2.5)	3.3	25	72	96
$z_3(0)$	52	51 (28)	38 (2.6)	2.7	27	75	97

* GSD: Geometric standard deviation

FIGURE CAPTIONS

Figure 1: Epidemiological model of *P. falciparum* malaria in humans (23). Compartments represent the four epidemiological classes considered in the human population. Arrows indicate transitions among compartments. Symbols are given in Appendix.

Figure 2: Time-course of *P. falciparum* daily prevalence (number of thick blood smears with positive trophozoites divided by the total number of smears) in 176 individuals living in Ndiop from the July 1 1993 to July 31 1994. The points correspond to observations. The thick line is the model-predicted prevalence in the population, as a function of time. It was obtained by running the model with the vector of parameter values having highest posterior density (among our random sample of 15000 posterior vectors). The thin lines are also model predictions of prevalence, generated with 10 other random parameter vectors drawn from their posterior distribution (see text). The outermost two lines correspond to the CI_{95} on predicted prevalence.

Figure 3: Model predictions of the fractions of the Ndiop human population in four epidemiological states for years 1993-1994 (thick lines: predictions obtained by running the model with the vector of parameter values having highest posterior density; thin lines: predictions generated with 10 random posterior parameter vectors; the outermost two lines correspond to the CI_{95} on predictions). The dotted lines correspond to the entomological inoculation rate (EIR) for the same period of time.

Figure 4: Model-reconstructed incidence rate of trophozoite parasitaemia in Ndiop population during the 1993 wet season. Thick solid line: incidence rate contributed by non-immune subjects; thick dashed line: contributed by immune subjects; thin line: EIR.

Figure 5: Model-predicted immunity acquisition and conversion delays as a function of the EIR. Computations were made with the parameter set having highest posterior density.

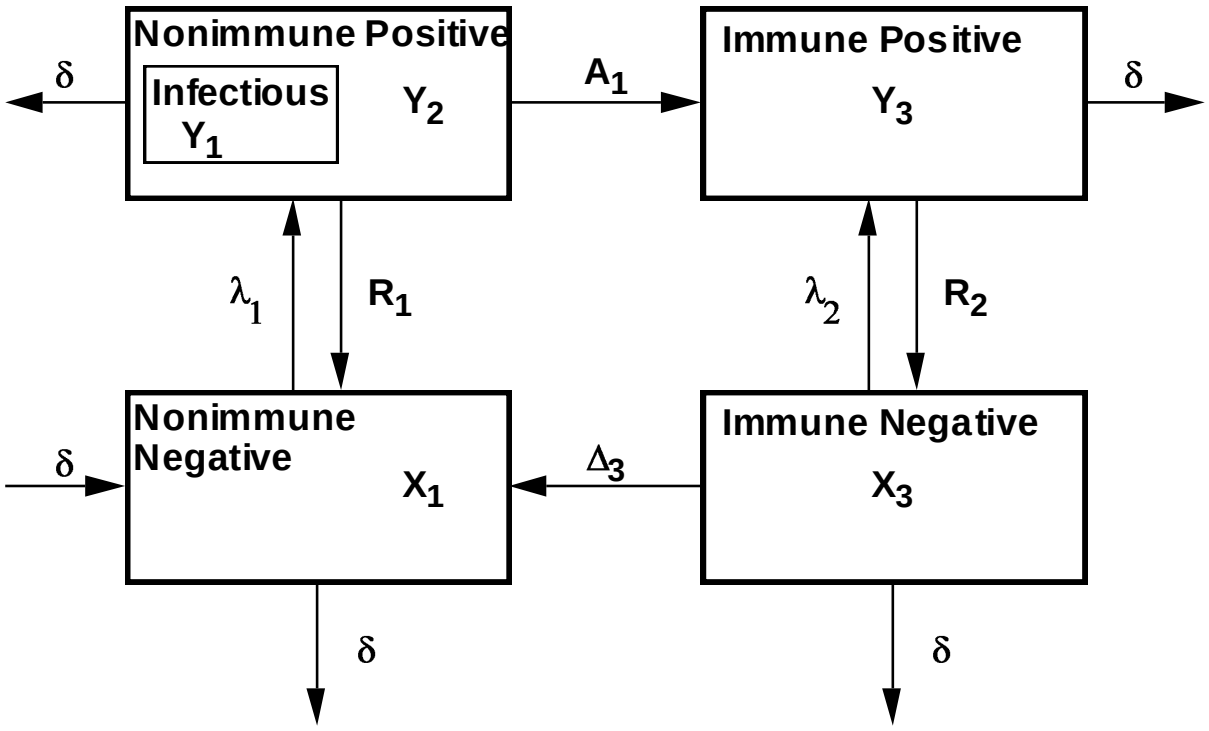

Figure 1: Epidemiological model of *P. falciparum* malaria in humans (23). Compartments represent the four epidemiological classes considered in the human population. Arrows indicate transitions among compartments. Symbols are given in Appendix.

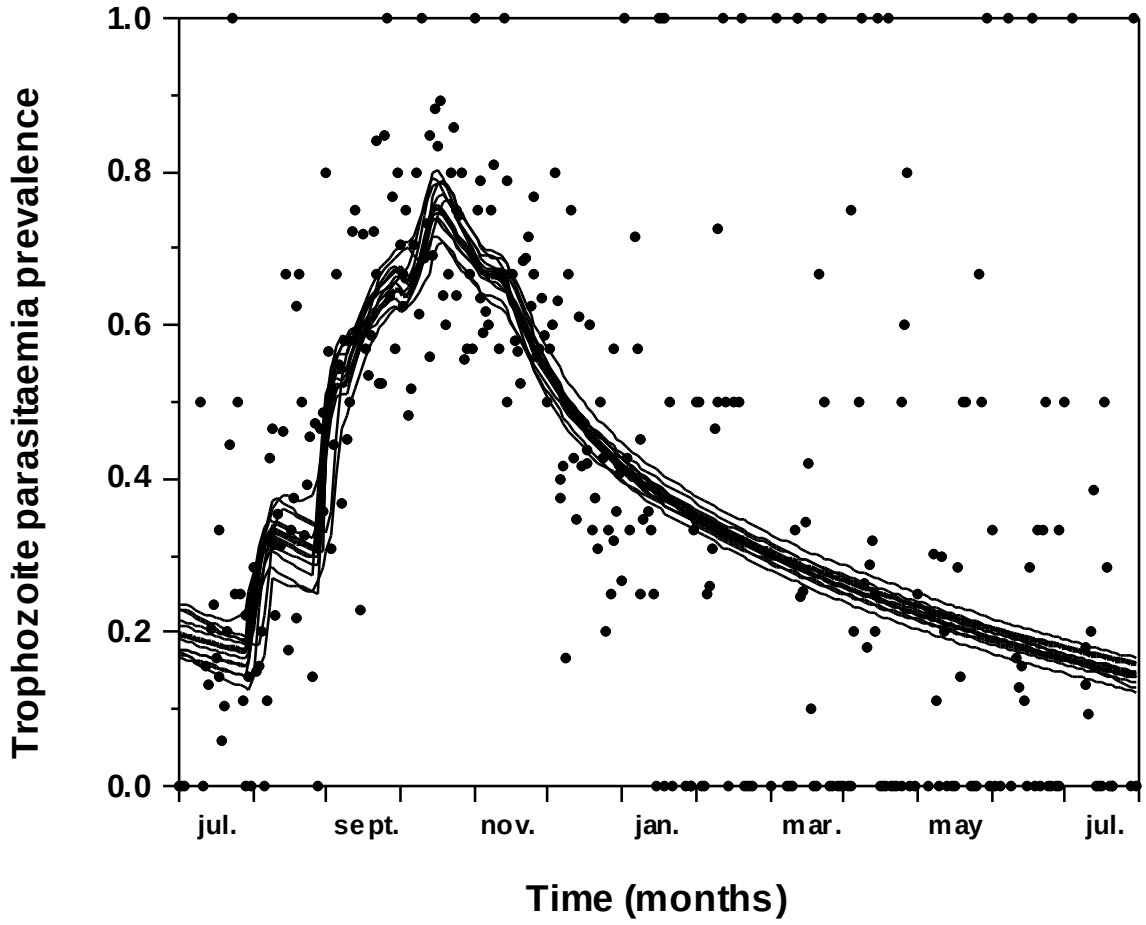

Figure 2: Time-course of *P. falciparum* daily prevalence (number of thick blood smears with positive trophozoites divided by the total number of smears) in 176 individuals living in Ndiop from the July 1 1993 to July 31 1994. The points correspond to observations. The thick line is the model-predicted prevalence in the population, as a function of time. It was obtained by running the model with the vector of parameter values having highest posterior density (among our random sample of 15000 posterior vectors). The thin lines are also model predictions of prevalence, generated with 10 other random parameter vectors drawn from their posterior distribution (see text). The outermost two lines correspond to the CI_{95} on predicted prevalence.

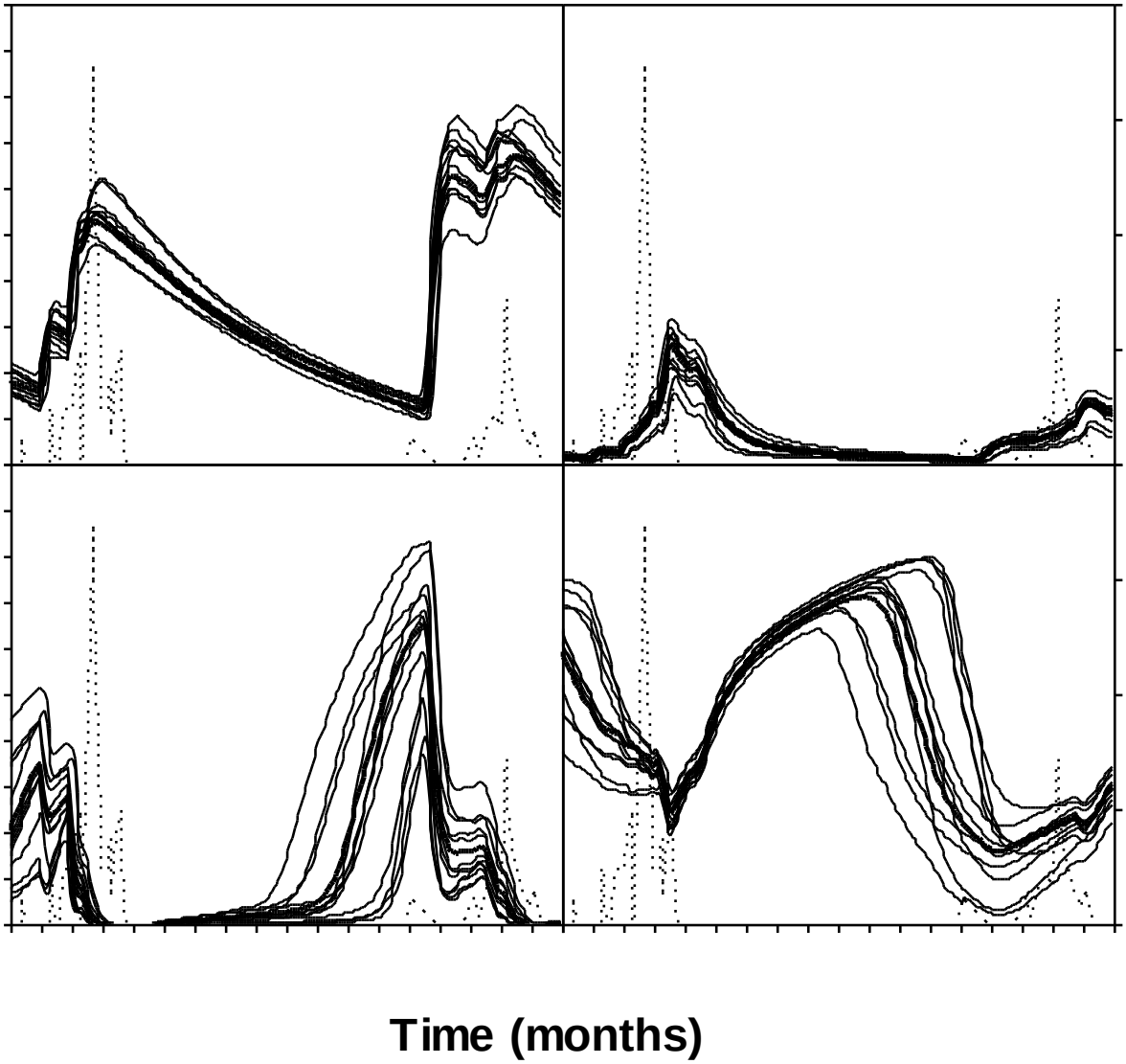

Figure 3: Model predictions of the fractions of the Ndiop human population in four epidemiological states for years 1993-1994 (thick lines: predictions obtained by running the model with the vector of parameter values having highest posterior density; thin lines: predictions generated with 10 random posterior parameter vectors; the outermost two lines correspond to the CI_{95} on predictions). The dotted lines correspond to the entomological inoculation rate (EIR) for the same period of time.

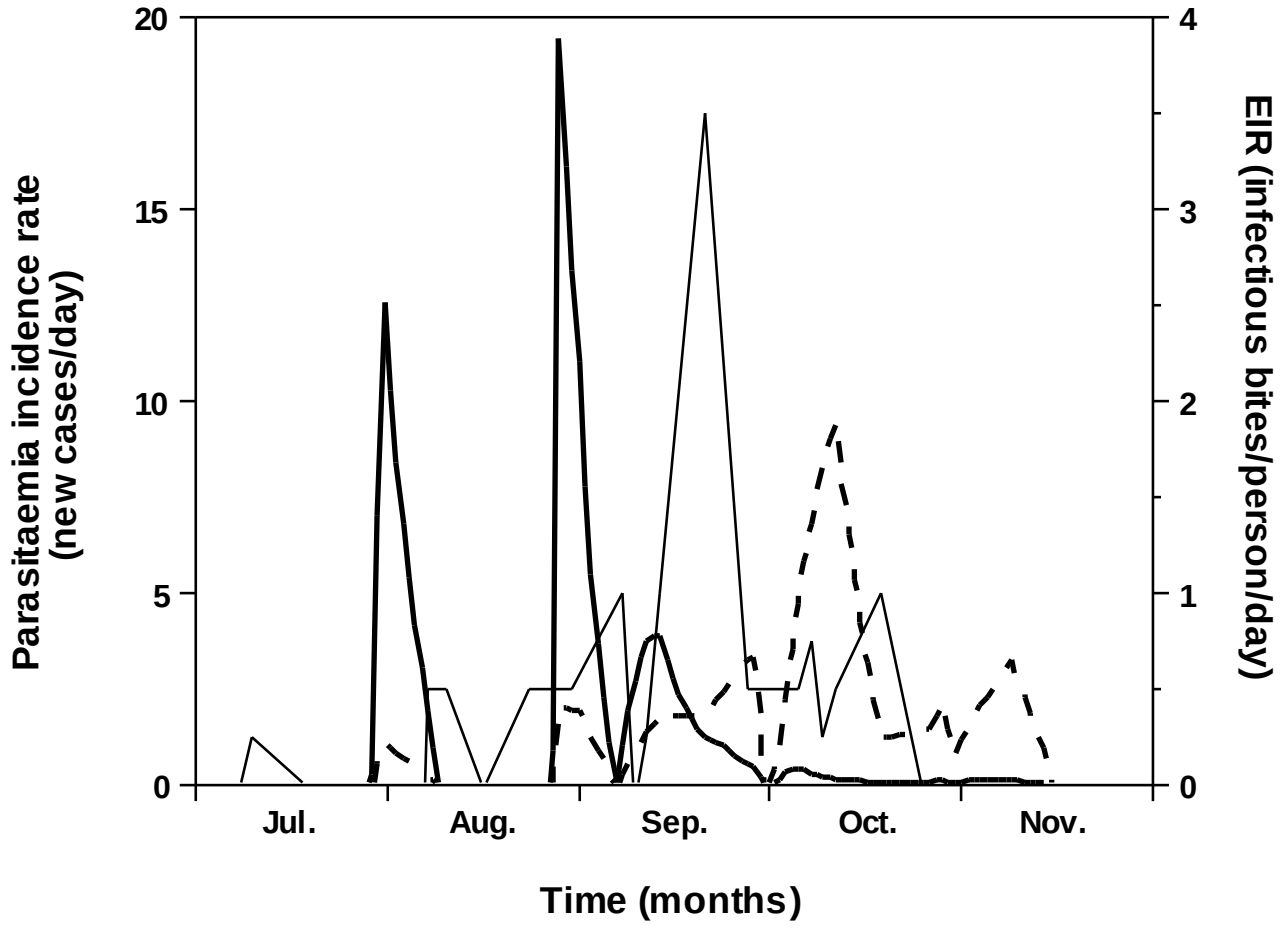

Figure 4: Model-reconstructed incidence rate of trophozoite parasitaemia in Ndiop population during the 1993 wet season. Thick solid line: incidence rate contributed by non-immune subjects; thick dashed line: contributed by immune subjects; thin line: EIR.

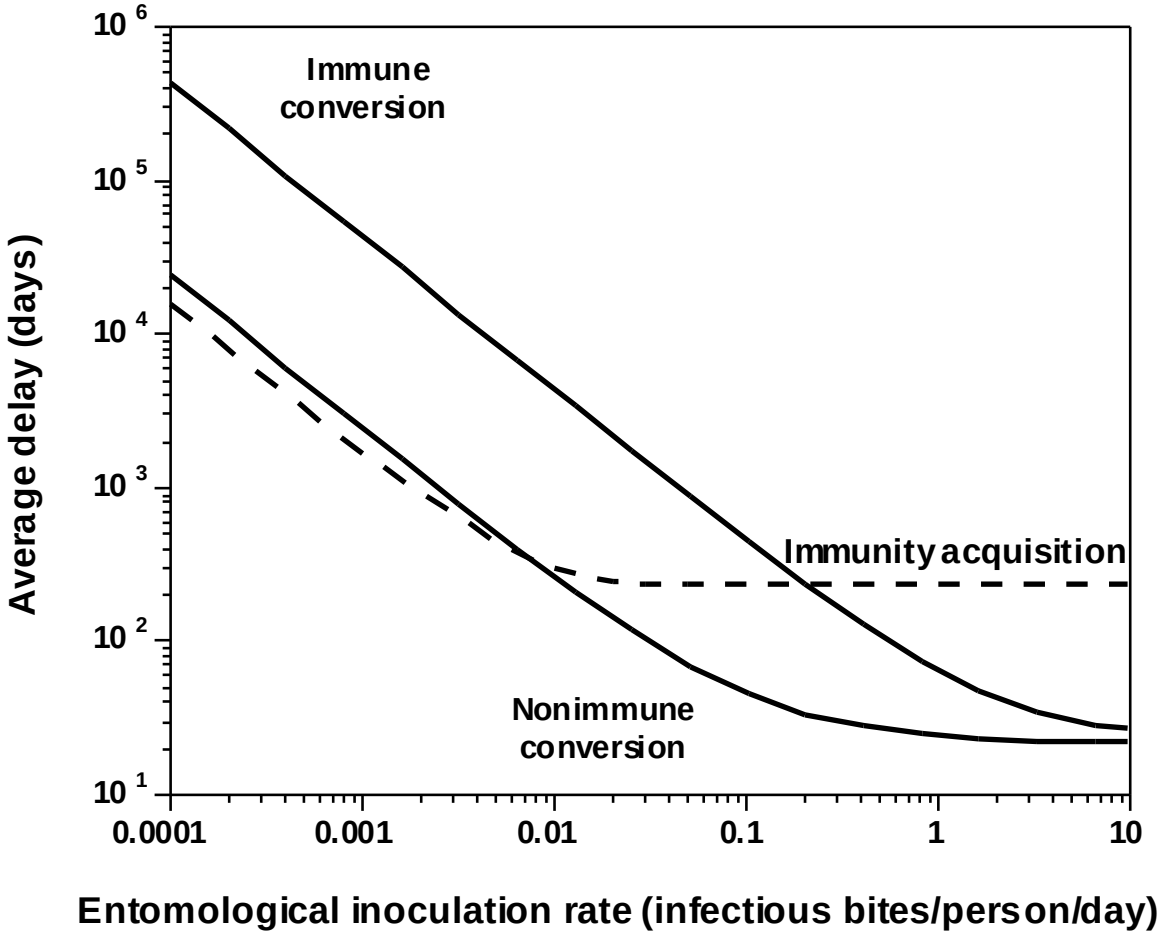

Figure 5: Model-predicted immunity acquisition and conversion delays as a function of the EIR. Computations were made with the parameter set having highest posterior density.